Simplicial closure and higher-order link prediction

Austin R. Benson[a], **Rediet Abebe**[a], **Michael T. Schaub**[b,c], **Ali Jadbabaie**[b], **and Jon Kleinberg**[a,1]

[a]Department of Computer Science, Cornell University, Ithaca, NY USA 14853; [b]Institute for Data, Systems, and Society, Massachusetts Institute of Technology, Cambridge, MA USA 02139; [c]Department of Engineering Science, University of Oxford, UK OX1 3PJ

This manuscript was compiled on October 24, 2018

Networks provide a powerful formalism for modeling complex systems by using a model of pairwise interactions. But much of the structure within these systems involves interactions that take place among more than two nodes at once—for example, communication within a group rather than person-to-person, collaboration among a team rather than a pair of coauthors, or biological interaction between a set of molecules rather than just two. Such *higher-order interactions* are ubiquitous, but their empirical study has received limited attention, and little is known about possible organizational principles of such structures. Here we study the temporal evolution of 19 datasets with explicit accounting for higher-order interactions. We show that there is a rich variety of structure in our datasets but datasets from the same system types have consistent patterns of higher-order structure. Furthermore, we find that tie strength and edge density are competing positive indicators of higher-order organization, and these trends are consistent across interactions involving differing numbers of nodes. To systematically further the study of theories for such higher-order structures, we propose higher-order link prediction as a benchmark problem to assess models and algorithms that predict higher-order structure. We find a fundamental differences from traditional pairwise link prediction, with a greater role for local rather than long-range information in predicting the appearance of new interactions.

higher-order | link prediction | network analysis | simplicial complex

Networks are a fundamental abstraction for complex systems and relational data throughout the sciences (1–3). The basic premise of network models is to represent the elements of the underlying system as nodes, and to use the links of the network to capture pairwise relationships. In this way, a social network can represent the friendships between pairs of people; a Web graph can encode links among Web pages or topic categories; and a biological network can represent the interactions among pairs of biological molecules or components (3–6). But much of the structure in these systems involves *higher-order interactions* between more than two entities at once (7–11): people often communicate or interact in social groups, not just in pairs; associative relations among ideas or topics often involve the intersection of multiple concepts; and joint protein interactions in biological networks are associated with important phenomena (12).

These types of higher-order, group-based interactions are apparent even in the standard genres of datasets used for network analysis. For example, coauthorship networks are built from data in which larger groups write papers together, and similarly, email networks are based on messages that often have multiple recipients. While such higher-order structure is not captured by the topology of a graph, it may be modeled via a collection of formalisms that include set systems (13), hypergraphs (14), simplicial complexes (15), and bipartite affiliation graphs (7, 16). Despite the existence of mathematical formalisms for higher-order structure, there is no unifying study that analyzes the basic higher-order structure of such datasets. This is in sharp contrast to other notions of "higher-order models" generalizing graph data, such as multiplex networks (17) and higher-order Markov chain models (18, 19), which are successful but still rooted in a pairwise representation paradigm. We study the complementary direction of group interactions, as outlined in the examples above, and use the term "higher-order model" in this sense.

A key reason for the lack of large-scale studies in higher-order models is that data is often collected directly in a network format, thus eliminating higher-order interactions already at the data-collection stage. Another reason is that analyzing higher-order interactions can be computationally challenging for large datasets. Consequently, despite their potential importance, little is known about organizational principles of higher-order structures within real-world datasets. For instance, one question that remains to be answered is whether higher-order interactions enable us to differentiate different kind of datasets, or whether higher-order properties are universal across datasets.

Here, we provide the first steps in the direction of promoting a broad, rigorous study of higher-order topological interactions across domains. To this end, we study the structure and temporal evolution of 19 datasets from a variety of domains that have higher-order interactions. We find that distinct patterns for different domains are immediately revealed with 3-way interaction features that are not available from the graph structure of the networks alone.

Motivated by the importance of triangular structures in network clustering and the theory of triadic closure in social networks (4, 20), we study an extension of this theory via *simplicial closure*, or the way in which groups of nodes evolve until eventually co-appearing in a higher-order structure. In

Significance Statement

Networks provide a powerful abstraction for complex systems throughout the sciences by representing the underlying set of pairwise interactions, but much of the structure within these systems involves interactions that take place among more than two nodes at once. While these higher-order interactions are ubiquitous, an evaluation of the basic properties and organizational principles in such systems is missing. Here we study 19 datasets from biology, medicine, social networks, and the Web, and characterize how higher-order structure emerges and differs between domains. We then propose a general framework for evaluating higher-order data models based on link prediction, a task in which we seek to predict future interactions from a system's structure and past history.

ARB, RA, MTS, AJ, and JK designed and performed research, analyzed data, and wrote the paper.

The authors declare no conflicts of interest.

[1]To whom correspondence should be addressed. E-mail: kleinber@cs.cornell.edu

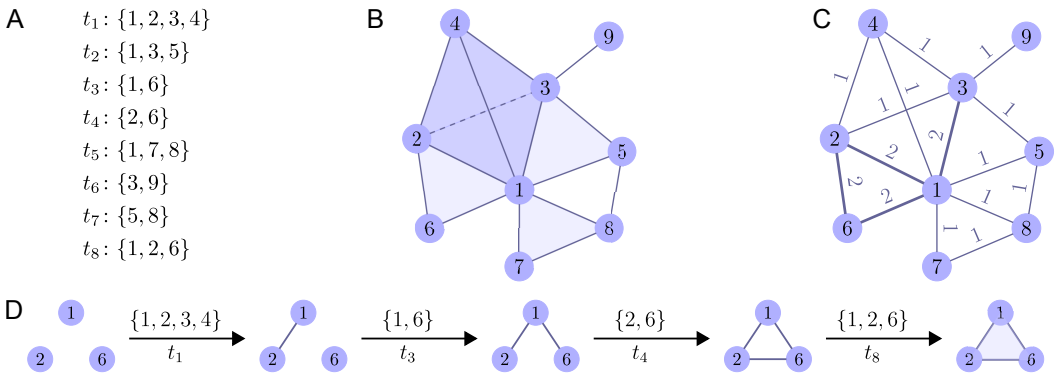

Fig. 1. Higher-order network models, open and closed closed 3-node cliques (triangles), and simplicial closure events. (**A**) Example higher-order network dataset consisting of eight timestamped simplices on nine nodes. More than one simplex can appear at a given time, which often occurs in real-world data with coarse-grained temporal measurements. We study 19 real-world datasets of this type (Table 1). (**B**) Visual representation of the dataset (ignoring timestamps). Shading represents the simplices (in order to highlight the difference with traditional graphs), and the dashed line between nodes 2 and 3 denotes three-dimensional perspective for the 4-node simplex $\{1, 2, 3, 4\}$ (this 4-node simplex also has darker shading). Nodes 1, 2, and 3 form a *closed* 3-node clique (i.e., closed triangle) since all three nodes appeared in the same simplex at time t_1, whereas nodes 1, 5, and 8 form an *open* triangle since all three pairs of nodes co-appeared in a simplex (time t_2 for nodes 1 and 5, time t_5 for nodes 1 and 8, and time t_7 for nodes 5 and 8) but no one simplex contains all three nodes. Thus, the region between nodes 1, 5, and 8 is not shaded. In total, the dataset has seven closed triangles—$\{1, 2, 3\}$, $\{1, 2, 4\}$, $\{1, 3, 4\}$, $\{2, 3, 4\}$, $\{1, 3, 5\}$, $\{1, 2, 6\}$, $\{1, 7, 8\}$—and one open triangle—$\{1, 5, 8\}$. We find that the fraction of triangles that are open varies widely depending on the dataset (Fig. 2). (**C**) The "projected graph" of the dataset. The weight of an edge is the number of times its two end points have appeared in a simplex together. Open and closed triangles are both triangles in the projected graph. Traditional network science ideas often ignore higher-order structure and only use this graph. (**D**) A simplicial closure event for nodes 1, 2, and 6. Each transition lists the new simplex and the time it appears in the dataset. Before closing, the three nodes induce several subgraphs in the projected graph over time. For example, the nodes form an open triangle at time t_4, which persists until time t_8 when the simplicial closure event occurs. We study properties of such simplicial closure events and predict their future occurrence as part of a framework for evaluating higher-order network models.

this case, we find that strong previous interactions between subsets of a group increases the likelihood of a *simplicial closure event*, where the nodes appear in a group together. The relative importance of different types of prior interactions depends on the dataset yet remains consistent when considering groups of different sizes for a given dataset. To facilitate future modeling and demonstrate that the higher-order patterns are not simple epiphenomena of the underlying link structure, we introduce a higher-order link prediction problem—the forecasting of future higher-order interactions—as an evaluation framework for models and algorithms that aim to predict the emergence of higher-order structure from existing data.

Structural analysis of higher-order networks

We assembled a diverse collection of 19 datasets, recording the timestamped interactions of groups of entities. Thus, each dataset is a set of timestamped sets of nodes. We call each set of nodes a *simplex*, and the nodes in each simplex take part in a shared interaction at a given timestamp (Fig. 1A). For example, in a coauthorship network, a simplex corresponds to a set of authors publishing an article at a given time.

Formally, each dataset consists of N timestamped simplices, $\{(S_i, t_i)\}_{i=1}^{N}$, where $t_i \in \mathbb{R}$ is the time at which simplex S_i was observed, and S_i is a set representing the nodes in the ith simplex. If $|S_i| = k$, we say that S_i is a k-node simplex.* This set-based representation provides a natural format for datasets from a range of domains. We briefly describe our datasets below (see *SI Appendix* for more complete descriptions).

- *Coauthorship data* (coauth-DBLP; coauth-MAG-History; coauth-MAG-Geology): nodes are authors and a simplex is a publication; DBLP spans over 80 years and the other two datasets span about 200 years.
- *Online tagging data* (tags-stack-overflow; tags-math-sx; tags-ask-ubuntu): nodes are tags (annotations) and a simplex is a set of tags for a question on online Stack Exchange forums; the data contains the complete history of the forums.
- *Online thread participation data* (threads-stack-overflow; threads-math-sx; threads-ask-ubuntu): nodes are users and a simplex is a set of users answering a question on a forum; again, the data contains the complete history of the forum.
- *Drug networks from the National Drug Code Directory* (NDC-classes): nodes are class labels (e.g., serotonin reuptake inhibitor) and a simplex is the set of class labels applied to a drug (all applied at one time). (NDC-substances): nodes are substances (e.g., testosterone) and a simplex is the set of substances in a drug; datasets include the complete history of the directory
- *U.S. Congress data* (congress-committees (21); congress-bills (22)): nodes are members of Congress and a simplex is the set of members in a committee or co-sponsoring a bill; the committees dataset spans 1989 to 2003 and the bills dataset spans 1973 to 2016.
- *Email networks* (email-Enron (23); email-Eu (24)): nodes are email addresses and a simplex is a set consisting of all recipient addresses on an email along with the sender's address; email-Enron spans most of the duration of a company's lifetime, and email-Eu spans over 2 years.
- *Contact networks* (contact-high-school (25); contact-primary-school (26)): nodes are persons and a simplex is a set of persons in close proximity to each other
- *Drug usage in the Drug Abuse Warning Network* (DAWN): nodes are drugs and a simplex is the set of drugs reportedly used by a patient prior to an emergency department visit.
- *Music collaboration* (music-rap-genius): nodes are rap artists; simplices are sets of rappers collaborating on songs.

To provide uniformity across datasets, we restrict to simplices consisting of at most 25 nodes. This is relevant to, e.g., the coauthorship data in which large consortia of hundreds of

*Such a structure is called a (k-1)-simplex in algebraic topology, and the set of all its pairs is called a k-clique in graph theory.

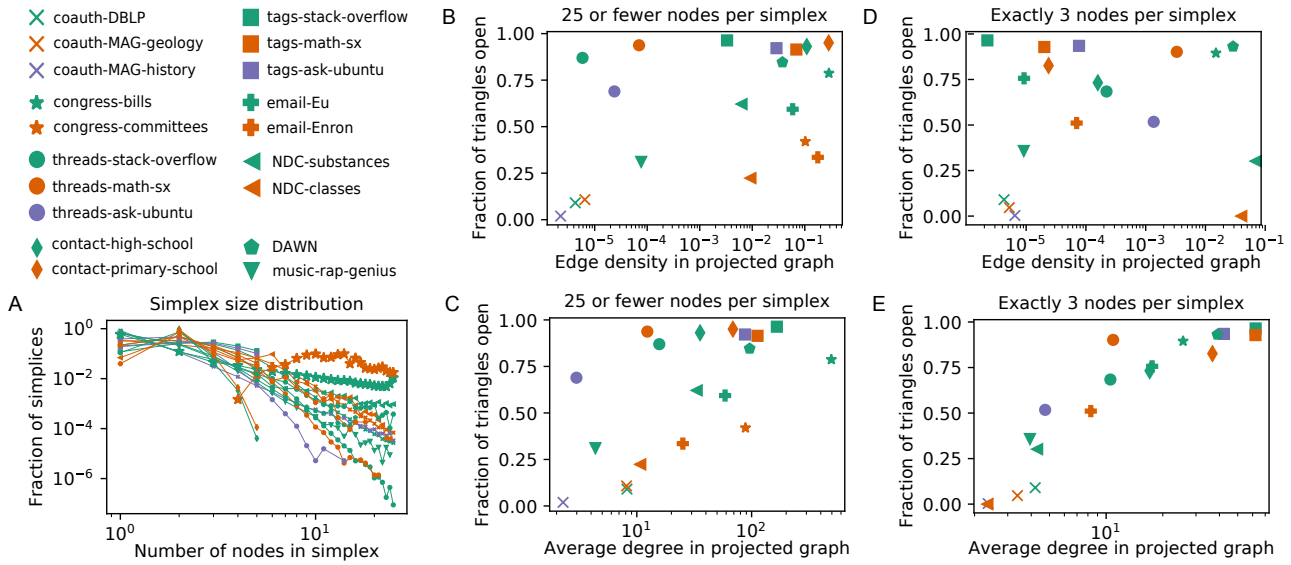

Fig. 2. Basic structure of higher-order interaction datasets. (**A**) Distribution of simplex sizes. In most datasets, small simplices (≤ 4 nodes) are the most common. (**B–C**) Dataset landscapes in terms of fraction of triangles that are open and either edge density (B,D) or average degree (C,E) when considering simplices with 25 or fewer nodes (B and C) or just 3-node simplices (D and E). Datasets from the same domain tend to be similar with respect to these features, whether or not we include simplices with greater than 3 nodes. Indeed, we can predict the system domain of some datasets by measuring these statistics on egonets (Table 2 and Fig. 3).

Table 1. Summary statistics for our datasets. Each dataset is a collection of timestamped simplices (as in Fig. 1).

Dataset	nodes	edges in proj. graph	timestamped simplices	unique simplices
coauth-DBLP	1,924,991	7,904,336	3,700,067	2,599,087
coauth-MAG-Geology	1,256,385	512,0762	1,590,335	1,207,390
coauth-MAG-History	1,014,734	1,156,914	1,812,511	895,668
music-rap-genius	56,832	123,889	224,878	85,429
tags-stack-overflow	49,998	4,147,302	14,458,875	5,675,497
tags-math-sx	1,629	91,685	822,059	174,933
tags-ask-ubuntu	3,029	132,703	271,233	151,441
threads-stack-overflow	2,675,955	20,999,838	11,305,343	9,705,709
threads-math-sx	176,445	1,089,307	719,792	595,778
threads-ask-ubuntu	125,602	187,157	192,947	167,001
NDC-substances	5,311	88,268	112,405	10,025
NDC-classes	1,161	6,222	49,724	1,222
DAWN	2,558	122,963	2,272,433	143,523
congress-bills	1,718	424,932	260,851	85,082
congress-committees	863	38,136	679	678
email-Eu	998	29,299	234,760	25,791
email-Enron	143	1,800	10,883	1,542
contact-high-school	327	5,818	172,035	7,937
contact-primary-school	242	8,317	106,879	12,799

authors collaborate on a single paper. However, such events are rare and not relevant for our analysis. Table 1 lists some summary statistics of the datasets The number of unique simplices appearing in the data is minuscule compared to the total number of possible simplices. For example, in the dataset with the smallest number of nodes (email-Enron, 143 nodes), there are nearly 500 million possible simplices of size at most 5, whereas only 1,542 unique simplices appear in the dataset. On the other hand, in most datasets, the number of unique simplices is within an order of magnitude of the number of pairs of nodes that co-appear in some simplex (edges in the projected graph; to be be discussed in the next section).

Higher-order features reveal rich structural diversity. Our data representation distinguishes between the observation of different kinds of k-way interactions between a set of entities. Stated differently, unlike in a graph representation, we do not break down each simplex into a set of (induced) pairwise interactions. Though the specific representation is not essential provided the information of the group interaction is faithfully encoded, it is convenient to think of our data as an abstract simplicial complex as depicted in Fig. 1B.

The simple encoding of the observed information as a graph is called the *projected graph*. Formally, in the projected graph, two nodes are joined by an edge of weight w if they co-appear in w simplices (Fig. 1C). A k-clique in the projected graph is a set of nodes among which an edge is present between all pairs. A k-cliques appear if (i) the k nodes were all part of a some simplex, or (ii) each pair was part of some simplex, although all k were never part of the same simplex. In the former case, we say the k nodes form a *closed* clique, while in the latter case we say they form an *open* clique.

We first study the occurrence of open and closed 3-cliques, or triangles (Fig. 2). This is the simplest higher-order structure present in our datasets that is not captured by a graph. Furthermore, triangles are one of the most important structural patterns in network analysis (4, 8, 27). As discussed above, there are two types of triangles which cannot be distinguished by the weighted projected graph alone. In a *closed triangle*, all three nodes have co-appeared in at least one simplex. Formally, $\{u, v, w\}$ is a closed triangle if there exists some simplex S_i for which $\{u, v, w\} \subset S_i$. In an *open triangle*, on the other hand, every pair of the three nodes has co-appeared in at least one simplex, but no single simplex contains all three nodes.

Every simplex with at least three nodes directly creates a closed triangle, while open triangles appear coincidental. Moreover, larger simplices lead to many closed triangles: for instance, a k-node simplex contributes $\binom{k}{3}$ closed triangles. Thus, one might intuit that closed triangles are much more common than open triangles due the presence of (potentially) large groups. On the other hand, only a small fraction of all possible simplices are present in the network when compared

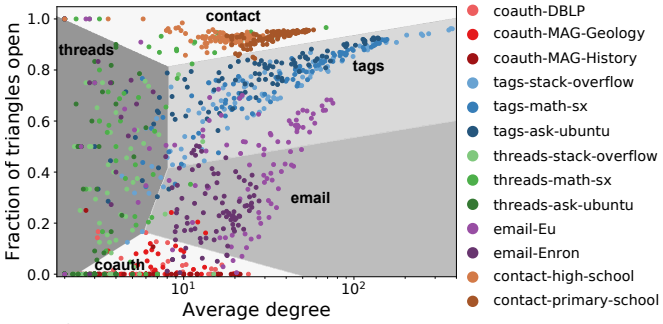

Fig. 3. Class decision boundaries of the learned multinomial logistic regression model for predicting five dataset system domains (coauthorship, threads, tags, email, or contact) using the log of the average degree ($\log(\bar{d})$) and fraction of triangles that are open (f) of egonets (Table 2 and *Materials and Methods*). Markers correspond to sampled egonets used in model training. The two-feature linear model can predict the 5-class dataset domain with 75% accuracy (Table 2). In conjunction with the prediction accuracies in Table 2, our analysis suggests that the fraction of triangles that are open (a higher-order network statistic) is an important covariate for analyzing and modeling the local structure of higher-order interaction data.

to the total number of possible edges in the projected graph, so one might expect that there are more open triangles. Our analysis reveals that, across our datasets, there is a spectrum for the fraction of triangles that are open (Figs. 2B and 2C).

While the distribution of simplex sizes is broadly similar in most datasets (Fig. 2A), jointly analyzing the edge density in the projected graph with the fraction of triangles that are open reveals a rich landscape of datasets (Fig. 2B): (i) low-density with a small fraction of triangles open (coauthorships and music collaboration); (ii) low-density with a large fraction of triangles open (stack exchange threads) (iii) high-density with a large fraction of triangles open (stack exchange tags, contact, bill co-sponsorship); and (iv) high-density with a medium fraction of triangles open (email, Congress committee membership, NDC substances and classes). These results are not skewed by large simplices—the landscape is broadly preserved when restricting to the 3-node simplices (Fig. 2D).

Measuring average unweighted degree along with fraction of open triangles also reveals substantial diversity, and datasets from the same domain continue to exhibit similar features (Fig. 2C). Restricting the data to only 3-node simplices, we find a near-linear relationship between the fraction of open triangles and the log of the average degree (Fig. 2E). A linear model for the data in Fig. 2E has $R^2 = 0.85$, compared to $R^2 = 0.38$ for a linear model of the data in Fig. 2D. This suggests that larger simplices bring diversity to the data.

Higher-order egonet features discriminate system domains. The structural diversity of the datasets is also present at the local level of egonets (1-hop neighborhoods of nodes), and local statistics can identify the "system domain" of datasets. By system domain, we simply mean the categories identified in Fig. 2 that correspond to datasets recorded from the same kind of system. Our collection of datasets has five clear system domains with at least two datasets each: coauthorship, online tags, online thread co-participation, email, and proximity contact. Using a multinomial logistic regression model to determine system domain with the fraction of triangles that are open and log of the average degree as covariates reveals clustering structure of the system domains (Fig. 3). This simple model can predict system domain with nearly 75% accuracy, compared to approximately 21% accuracy with random guessing. The prediction accuracy provides evidence

Table 2. Prediction of dataset type by egonet features. For the datasets from coauthorship, threads, tags, email, and contact system domains, we sampled egonets and computed the edge density (ρ), average degree ($\bar{d}$), and fraction of triangles that are open (f). Using these features, we trained a multinomial logistic regression model to predict the system domain of the network (see *Materials and Methods*). Models incorporating the fraction of triangles that are open outperform the one that does not, highlighting the importance of this feature for higher-order organization. Figure 3 illustrates the model that uses $\log(\rho)$ and f as features.

model features				accuracy	
$\log(\rho)$	$\log(\bar{d})$	f	intercept	random	multinomial LR
X	X	X	X	0.21	0.78 ± 0.02
	X	X	X	0.21	0.75 ± 0.02
X		X	X	0.21	0.60 ± 0.02
X	X		X	0.21	0.49 ± 0.03

that there are different organizational mechanisms at play locally for different systems. In conjunction with the structure illustrated in Fig. 2, this suggest that there is not a single "universal" setting of values for simplicial network statistics; the context of the underlying the network matters, but within a given context the parameters are quite stable.

We also trained models with the log of the edge density as a covariate, in addition to the log of the average degree and the fraction of triangles that are open; model accuracy mildly increased from 75% to 78% (Table 2). However, discarding the log of the average degree as a covariate decreases model accuracy to 60%, and only including edge density and average degree without the fraction of triangles that are open decreases model accuracy to 50%. The accuracy numbers are guides in how to model higher-order interaction data. For example, we conclude that the fraction of triangles that are open—a network statistics that relies on knowledge of the higher-order structure in the dataset—is a valuable covariate for identifying system domains. Thus, simple higher-order interactions should be used when analyzing or modeling such data. Furthermore, the average degree tends to be more valuable than edge density when considering local organizational mechanisms.

A simple generative model for open and closed triangles. We have now seen that there is diversity in datasets from global network statistics and that local statistics reveal system domains of the networks. We now provide a simple generative model of simplices that helps describe how diversity in the datasets might arise. The model uses the hypothesis that 3-node simplices form independently with a fixed probability. While extreme, this hypothesis indeed leads to diversity in the fraction of triangles that are open. To see this, suppose that a dataset consists only of 3-node simplices on n nodes, and any set of three nodes $\{u, v, w\}$ appears in a simplex with probability $p = 1/n^b$, where $b > 0$ is a parameter regulating the probability of this event. Let X_{uvw} be the indicator random variable that $\{u, v, w\}$ is an open triangle. Then, for large n, it follows from the independence assumption that

$$\mathbb{E}[X_{uvw}] \approx (1 - (1 - 1/n^b)^n)^3. \qquad [1]$$

There are two asymptotic regimes here depending on the value of b. If $b < 1$, then $(1 - 1/n^b)^n \leq e^{-n^{1-b}}$, and $\mathbb{E}[X_{uvw}]$ approaches 1 as n gets large. If $b > 1$, on the other hand,

$$\mathbb{E}[X_{uvw}] \approx (1 - (1 - 1/n^b)^n)^3 = O(1/n^{3b-3}). \qquad [2]$$

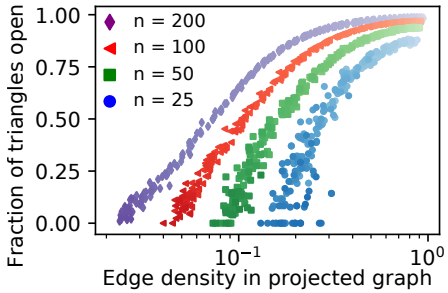

Fig. 4. Distribution of the fraction of triangles that are open and edge density in simulations from a model where each triple of n total nodes forms a 3-node simplex independently with probability $p = 1/n^b$, $b \in [0.8, 1.8]$. Color scales with b so that larger p are lighter and smaller p are darker. Varying b creates datasets spanning all possible values of the fraction of triangles that are open.

Denote the set of open triangles by $\mathcal{O}$ and the set of closed triangles by $\mathcal{C}$. According to our calculations above, for large n, the expected number of open triangles is $\mathbb{E}[|\mathcal{O}|] = \sum_{\{u,v,w\}} \mathbb{E}[X_{uvw}] = O(n^3)$ if $b < 1$. For $b > 1$, the expected number of open triangles for large n is $\mathbb{E}[|\mathcal{O}|] = O(n^{3(2-b)})$. The expected number of closed triangles is always $\mathbb{E}[|\mathcal{C}|] = p \cdot \binom{n}{3} = O(n^{3-b})$. Therefore, if $b < 3/2$, the number of open triangles grows faster, and if $b > 3/2$, the number of closed triangles grows faster. To illustrate this numerically, we generated 5 random samples from this model for $b = 0.8, 0.82, 0.84, \ldots, 1.8$ and $n = 25, 50, 100, 200$. As suggested by the above theory, the samples have a fraction of open triangles spanning the interval between 0 and 1 (Fig. 4).

We can also use the above procedure to construct datasets with a smaller edge density, while keeping the average degree fixed by patching together c replicates of one of these random datasets; this creates a dataset with c times as many nodes, but the same average degree. More formally, if a dataset with n nodes has average degree d and edge density ρ, then the union of c copies of this dataset has cn nodes, average degree d, and edge density $c\rho\left(\binom{n}{2} - n\right)/\left(\binom{nc}{2} - nc\right) \approx \rho/c$ (for large n). Thus, our simple independent model spans the two-dimensional feature space in Figs. 2B and 2D, but this does not imply that our data was generated by this model.

Temporal dynamics and simplicial closure events

The above analysis already reveals useful information about the organization of closed and open triangles, and studying the temporal dynamics of the networks in detail offers additional insights. A possible hypothesis for strong prevalence of open triangles would be temporal asynchrony in link creation. For example, consider three Congresspersons u, v, and w in the committee membership dataset, where u is in one committee with v and in another committee with w. If u is not re-elected, there will be no opportunity for the triple of nodes to form a closed triangle, as u has effectively become inactive. An open triangle may still form if v and w are on the same committee in a future Congress. However, we find that temporal asynchrony does not explain most open triangles. Depending on the dataset, the three edges in 61.1% to 97.4% of open triangles have an overlapping period of activity (including 89.5% for Congress committees; see *SI Appendix*).

Regardless of how open triangles are created, the three associated nodes may of course appear together in a simplex in the future as the network evolves. Deviating from our above simple model of independent creation of closed triangles, we find that many newly formed simplices in our data consist of k nodes that had previously constituted an open k-clique in the projected graph. We say that the appearance of a new simplex containing these k nodes is an instance of a *simplicial closure event*, i.e., the conversion of an open structure to a closed one, as illustrated in Fig. 1D.[†] In the following, we investigate the simplicial closure mechanism as an organizational principle for higher-order interactions.

Simplicial closure on triangles reveals competing features. Though conceptually similar, three nodes participating in a simplicial closure event is distinct from the well-known phenomenon of *triadic closure events* in social networks (4). A triadic closure event modifies the structure of the underlying pairwise interactions, whereas a simplicial closure event adds a new higher-order interaction without necessarily changing the pairwise structure of the projected graph.

Any induced subgraph on three nodes in the weighted projected graph can change several times before the three nodes appear in a simplex together, i.e., go through a simplicial closure event (Fig. 5). We call this the *lifecycle* of the triple of nodes. There are two changes that a triple of nodes can undergo during its lifecycle before a simplicial closure event. First, a new pairwise link can be added between two nodes u and v. This corresponds to an increase in density in this induced subgraph, e.g., the introduction of the drug Promacta adds an edge in Fig. 5B. Second, the projected graph edge weight between nodes u and v can increase, which we interpret as an increase in tie strength. For instance, in Fig. 5C, the tie strength between Gucci Mane and Young Thug increases after they collaborate on "Fell." To simplify our analysis, we differentiate only between *weak ties* corresponding to a single interaction ($W_{uv} = 1$ in the projected graph; denoted "1") and *strong ties* corresponding to multiple interactions over time ($W_{uv} \geq 2$; denoted "2+"). With this binning, there are 11 possible states in a lifecycle (Fig. 5A).

To get a first impression of the magnitude of these events, we examine the lifecycle of every triple of nodes that becomes an open or closed triangle in the coauth-MAG-History dataset (Fig. 5A). In this dataset, a closed triangle is more likely to have come from a configuration with exactly two strong ties edges (3,171 cases) than from an open triangle (328 + 779 + 722 + 285 = 2,114 cases). Most closed triangles are formed by nodes that had no previous interaction (2,732,839 cases); however, since the graph is sparse, the *fraction* of triples of nodes with no prior engagement that go through a simplicial closure event is small (see *SI Appendix*). Additionally, if three nodes induce an open triangle with only weak ties at some point in time, then the three nodes are more likely to gain a strong tie before closure (445 cases) than to close directly from that state (328 cases).

We also analyze the probability of a simplicial closure event conditioned on the state of the three nodes in its lifecycle. To do so, we split each dataset based on the temporal order of appearance of the simplices into a training set, consisting of the first 80% of the simplices (in time) and a test set of the remaining 20% of the simplices. Formally, if t_* is the 80th percentile of the timestamps $t_1, \ldots, t_N$, then the training set is the set of timestamped simplices $\{(S_i, t_i) \mid t_i \leq t_*\}$ and the test set consists of $\{(S_i, t_i) \mid t_i > t_*\}$. We then measured the probability that a triple of nodes from the training set is

[†] Here we are building on terminology for datasets of static sets of simplices (28). The term "simplicial closure" also appears in the combinatorial topology literature but with a different meaning (29).

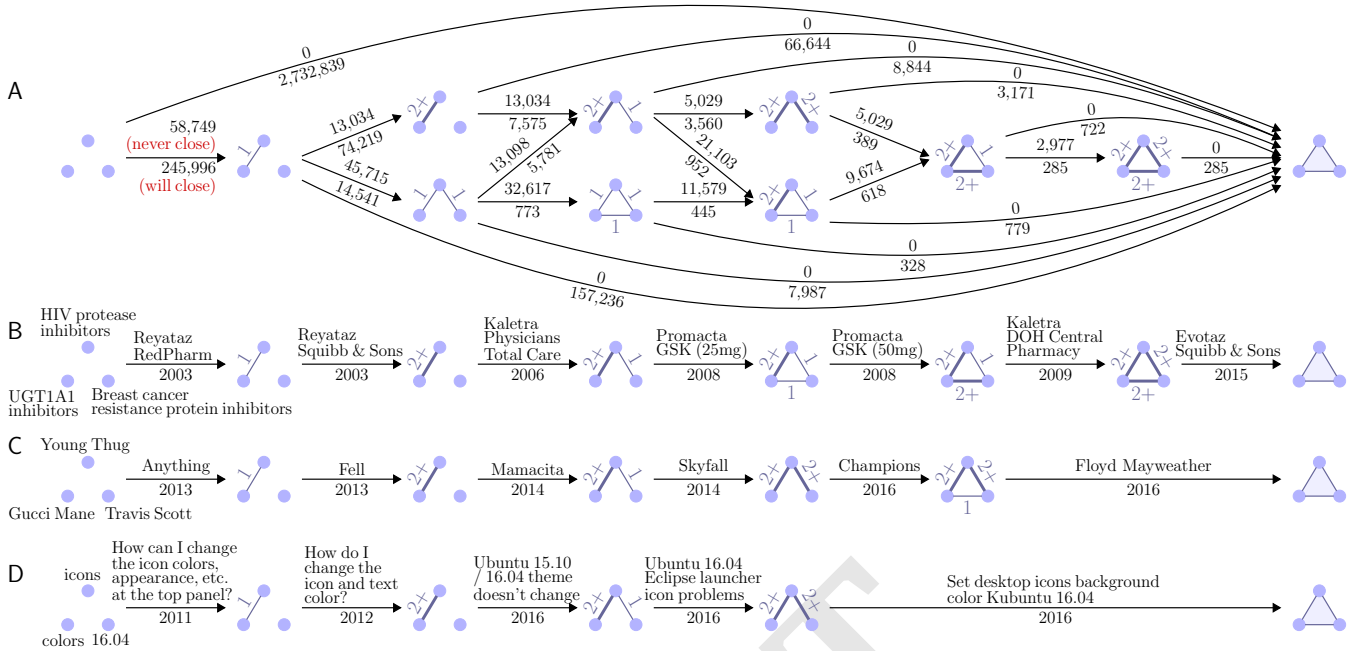

Fig. 5. Lifecycles of triples of nodes. Triangle edge weights are from the projected graph binned into weak ties for pairs of nodes appearing in only one simplex together (denoted "1") and strong ties for pairs of nodes appearing at least two simplices together (denoted "2+"). (**A**) Lifecycles in the coauth-MAG-History dataset for all triples that eventually form a triangle. Edges represent transitions between configurations, and the numbers are counts of triples that follow the transition. The top number counts triples of nodes that never experience simplicial closure event (i.e., never reach the closed state on the far right), and the bottom number counts triples that do go through a simplicial closure event. (**B**) Lifecycle of classification codes "HIV protease inhibitors", "UGT1A1 inhibitors", and "Breast cancer resistance protein inhibitors" in the NDC-classes dataset, where simplices consist of the labels applied to drugs. Reyataz and Kaletra—two HIV-1 medications—produced strong ties via multiple drug labelers; RedPharm Drug Inc. and E.R. Squibb & Sons, LLC labeled Reyataz, and Physicians Total Care and DOH Central Pharmacy labeled Kaletra. Promacta, a bone marrow stimulant classified as both a breast cancer resistance protein inhibitor and a UGT1A1 inhibitor, creates the open triangle. A strong tie is due to GlaxoSmithKline plc labeling multiple dosages of Promacta as products (25mg and 50mg). The introduction of Evotaz, a combination drug, induces a simplicial closure event for the three labels, 6 years after the open triangle formed. (**C**) Lifecycle of rap artists Young Thug, Gucci Mane, and Travis Scott. Mane and Thug first collaborated on the song "Anything" on a Mane mixtape; the two subsequently both featured on Waka Flocka Flame's track "Fell". Thug then twice featured on Travis Scott's 2014 mixtape "Days Before Rodeo", on the tracks "Mamacita" and "Skyfall". Both Mane and Scott featured on Kanye West's ensemble track "Champions," leading to an open triangle. A simplicial closure event occurred when Scott and Mane both featured on Thug's track "Floyd Mayweather." (**D**) Lifecycle of tags "icons", "colors", and "16.04" applied to questions on the Ask Ubuntu question-and-answer forum. The tag 16.04 refers to a 2016 Ubuntu release. There are questions about icons and colors independent of the Ubuntu version, dating back to 2011 (just one year after the forum was created). In 2016, users asked 16.04-specific icon questions related to the new release. Finally, a 16.04-specific question on both icons and colors leads to a simplicial closure event.

a closed triangle in the test set as a function of its previous configuration in the weighted projected graph, i.e., its lifecycle state in the training data (*SI Appendix* contains all of the simplicial closure event probabilities).

We highlight four important findings. First, the simplicial closure event probability typically increases with additional edges (Fig. 6A). In other words, as the edge density of the subgraph induced by the three nodes increases, the probability of a simplicial closure event increases. We formally test this by comparing the closure probability of a fixed weighted induced subgraph configuration and the same configuration with an additional unit-weight edge for all suitable cases. The latter has a statistically significant larger simplicial closure event probability in 102 of 113 cases over all datasets and pairs of configurations, whereas the less dense structure is never significantly more likely to close ($p < 10^{-5}$; see *Materials and Methods*). (Our goal here is to illustrate general trends rather than to find a single statistically significant result.) This result is consistent with both theoretical (4) and empirical (30) studies of dyadic link formation in social networks. However, several of our datasets are not social networks.

Second, the probability of a simplicial closure event typically increases with tie strength (Fig. 6B). We test the effect of tie strength by comparing the closure probability of a fixed weighted induced subgraph containing at least one weak tie, and the same configuration where the weak tie is converted to a strong tie. Increasing the tie strength significantly increases the probability of a simplicial closure event in 82 of 113 cases over all datasets and significantly decreases the closure probability in just 6 of 113 cases ($p < 10^{-5}$). Again, this result is consistent with both theoretical (4) and empirical (27, 31) studies of social networks, even though not all of our networks are social.

Third, neither edge density nor tie strength dominates the likelihood of simplicial closure events (Fig. 6C). In the coauthorship and Congress datasets, an open triangle comprised of three weak ties is more likely to close than a 3-node subgraph with just two strong ties. The reverse is true for the stack exchange tags and stack exchange threads datasets. Overall, the open triangle of weak ties is significantly more likely to close than the three nodes with two strong ties in 4 of 19 datasets, whereas the opposite is true in 6 of 19 datasets ($p < 10^{-5}$).

Fourth, the results reveal varying closure dynamics over the dataset domains. In human social interactions, simplicial closure events appear to be driven by a topological form of triadic closure: mutual acquaintance between all the nodes in a set increases the probability of a joint interaction. In contrast, simplicial closure events in the discussion platform networks resemble transitive closure: once there is a sufficiently strong

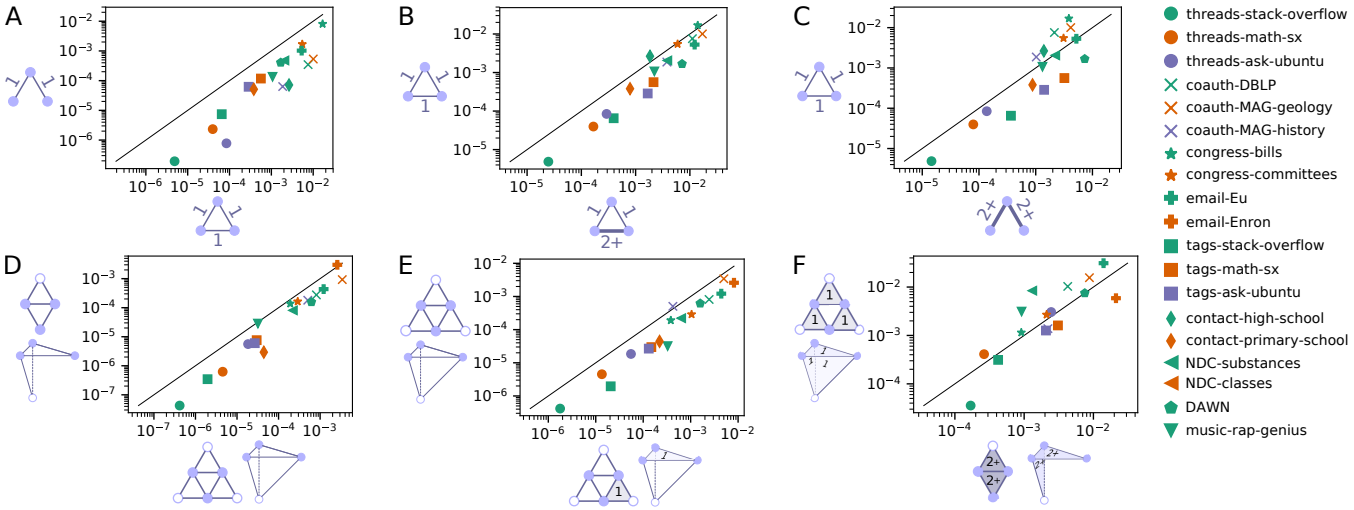

Fig. 6. Comparison of simplicial closure event probabilities based on configurations of 3-node and 4-node structures. The simplices appearing in the first 80% of the time spanned by the dataset determine the configuration (appearing as the x-axis and y-axis labels). The scatter plots compare the probability of different configurations going through a simplicial closure event in the final 20% of timestamped simplices. (**A–C**) Comparison of simplicial closure event probabilities for pairs of 3-node configurations that demonstrate how increasing edge density (A) or tie strength (B) increases the probability of a simplicial closure event. However, the relative importance of edge density and tie strength depends on the dataset (C). (**D–F**) Comparison of simplicial closure event probabilities for pairs of 4-node configurations. Each axis has two labels giving two pictorial representations of the configuration. The white node in the "flat" representation (left label on x-axis; top label on y-axis) represents the same node, so the 3-dimensional structure can be envision by folding the white nodes on top of each other. The other representation (right label on x-axis; bottom label on y-axis) shows a three-dimensional tetrahedral perspective of this folding. We again see that increasing edge density (D) or tie strength (E) increases the probability of a simplicial closure event. Here, "tie strength" is measured at the level of 3-node simplices, i.e., how often three nodes have appeared in a simplex (no times—not shaded; one time—shaded, denoted "1"; or at least two times—shaded, denoted "2+"). The relative importance of edge density and tie strength depends on the dataset but is consistent with the 3-node case. In three of the five datasets for which the configuration on the y-axis in (F) is significantly more likely to go through a simplicial closure event, the open triangle of weak ties is also significantly more likely to close for sets of three nodes (coauth-DBLP, coauth-MAG-Geology, congress-bills; c.f. (C); $p < 10^{-5}$). And in three of the four datasets for which the configuration on the x-axis in (F) is significantly more likely to go through a simplicial closure event the configuration with just two strong ties is also more likely to close than the open triangle with all weak ties (tags-stack-overflow, tags-math-sx, tags-ask-ubuntu; c.f. (C); $p < 10^{-5}$). Moreover, there were no datasets for which tie strength was significantly more indicative of simplicial closure events for one simplex size and density was more important for another (significance level 10^{-5}).

co-occurrences of tags, they become likely to be used together.

A possible concern with our analysis is that we only measured closure probabilities at one point in time for each dataset. Furthermore, while some of our datasets represent a complete history of the network (tags, threads, NDC) and some span a long duration of time (coauthorship, music, congress-bills), a few only contain a slice of the underlying network's dynamics (email-Eu, contact). However, we find that the closure probabilities and the results on edge density and tie strength are consistent at different points in time (see *SI Appendix*).

Simplicial closure properties extend beyond triangles. All four of the above findings hold for simplicial closure events on four nodes, so our results are not limited to structure on three nodes (Figs. 6D to 6F). Now, a simplicial closure event is all four nodes appearing in a simplex, and "tie strength" is measured on 3-node simplices, i.e., how often the 3-node subsets of a 4-node structure have appeared together in a simplex (0, or "open"; 1, or "weak"; at least 2 times, or "strong").

To measure the effect of edge density, we compare the closure probability of a configuration consisting of a fixed number of edges to the closure probability of the same configuration with an additional edge, keeping the tie strengths fixed (Fig. 6D shows one such comparison). In 180 of 228 applicable comparisons over all datasets, the closure probability significantly increases with the edge density and significantly decreases in only 2 cases ($p < 10^{-5}$). To measure the effect of tie strength, we compare the closure probability of a given configuration to the closure probability of the same configuration where the tie strength increases from an open tie to a weak tie or from a weak tie to a strong tie (Fig. 6E shows a case where the tie strength increases from open to weak). The closure probability significantly increases with simplicial tie strength in 26 of 38 cases for 3-edge configurations, 31 of 38 cases for 4-edge configurations, 77 of 114 cases for 5-edge configurations, and 177 of 359 cases for 6-edge configurations; compared to a significant decrease in closure probability in just 2 of 38, 1 of 38, 1 of 114, and 4 of 359 cases ($p < 10^{-5}$). Therefore, tie strength is also a positive indicator of simplicial closure in 4-node configurations.

There is also tension between the influence of sparser configurations with strong ties and denser configurations with weak ties. Figure 6F shows one such comparison. In this case, three out of five datasets for which edge density is significantly more indicative than tie strength in the 3-node comparison of Fig. 6C, edge density is also significantly more important in the 4-node case ($p < 10^{-5}$). And in three of the four datasets for which tie strength is significantly more indicative than edge density in the same 3-node case, the same is true in the 4-node case. Finally, there is no dataset for which tie strength was significantly more influential for one simplex size and density was significantly more influential for another.

Higher-order link prediction

Thus far, we have showed that higher-order interactions provide a rich source of additional information beyond traditional network modeling. Our analysis leaves open many questions, such as the development of better mechanistic models for the emergence of these interactions. To facilitate this process, we propose an analog of link prediction for higher-order structure.

Table 3. Open triangle closure prediction performance based on eight models: harmonic, geometric, and arithmetic means of the 3 edge weights; 3-way Adamic-Adar coefficient (A-A); preferential attachment (PA); Katz similarity; personalized PageRank similarity (PPR); and a feature-based supervised logistic regression model (Log. reg.). Performance is AUC-PR relative to the random baseline, i.e., relative to the faction of open triangles that close. The top performance number for each dataset is bolded.

Dataset	Harm. mean	Geom. mean	Arith. mean	A-A	PA	Katz	PPR	Log. reg
coauth-DBLP	1.49	1.59	1.50	1.60	0.74	1.51	1.83	**3.37**
coauth-MAG-History	1.69	2.72	3.20	5.82	2.49	3.40	1.88	**6.75**
coauth-MAG-Geology	2.01	1.97	1.69	2.71	0.97	1.74	1.26	**4.74**
music-rap-genius	5.44	**6.92**	1.98	2.10	2.15	2.00	2.09	2.67
tags-stack-overflow	**13.08**	10.42	3.97	6.63	2.74	3.60	1.85	3.37
tags-math-sx	9.08	8.67	2.88	6.34	2.81	2.71	1.55	**13.99**
tags-ask-ubuntu	12.29	**12.64**	4.24	7.51	5.63	4.15	2.54	7.48
threads-stack-overflow	23.85	**31.12**	12.97	3.19	3.89	11.54	4.06	1.53
threads-math-sx	20.86	16.01	5.03	23.32	7.46	4.86	1.18	**47.18**
threads-ask-ubuntu	78.12	**80.94**	29.00	30.82	6.62	32.31	1.51	9.82
NDC-substances	4.90	5.27	2.90	5.97	4.46	2.93	1.83	**8.17**
NDC-classes	**4.43**	3.38	1.82	0.99	2.14	1.34	0.91	0.62
DAWN	4.43	3.86	2.13	**4.77**	1.45	2.04	1.37	2.86
congress-committees	3.59	3.28	2.48	5.04	1.31	2.59	3.89	**7.67**
congress-bills	0.93	0.90	0.88	0.66	0.55	0.78	1.07	**107.19**
email-Enron	1.78	1.62	1.33	0.87	0.83	1.28	**3.16**	0.72
email-Eu	1.98	2.15	1.78	1.37	1.55	1.79	1.75	**3.47**
contact-high-school	3.86	**4.16**	2.54	2.00	1.13	2.53	2.41	2.86
contact-primary-school	5.63	6.40	3.96	3.21	0.94	4.02	4.31	**6.91**

Model evaluation framework. The basic premise in link prediction—whether pairwise or higher-order—is to use structural network properties up to some time t to predict the appearance of new interactions after t. In traditional network analysis, link prediction is a cornerstone problem and a highly successful evaluation framework for comparing different models via a well-calibrated prediction task (32, 33). Specifically, link prediction examines data that evolves over time and sees how well a given model predicts the appearance of new links—for example, new coauthorships appearing in a coauthor network, or new messages between pairs of people in an email network.

In this context, a *model* is interpreted broadly and may be mechanistic (e.g., preferential attachment (34)), statistical (e.g., probabilistic hierarchical models (35)), or implicitly encapsulated by a principled heuristic algorithm. For instance, personalized PageRank is a model capturing the fact that a large number of walks between two nodes drives up the connection probability between them (32). A key advantage of link prediction as an evaluation framework is precisely that it can handle these various kinds of models. This holds even in the absence of a likelihood expression, which would be required for a more standard statistical evaluation of goodness of fit. While ultimately we may want to arrive at a generative, causal description of the emergence of higher-order patterns, the flexibility of link prediction enables us to probe the importance of features of the network data in a simple manner without having to create a formal statistical model.

Link prediction has proved valuable both for methodological reasons and also in concrete applications. Methodologically, asking whether one model is better than another at predicting new links provides a data-driven way of assessing the effectiveness of the models (32, 36, 37). Link prediction also has a number of direct applications that cut across disciplines, including predicting friendships in social networks (38), inferring new relationships between genes and diseases (39), and suggesting novel connections in the scientific community (40).

Link prediction is also used within model selection tools for evaluating community detection algorithms (41, 42). In these cases, link prediction may be interpreted as the smallest possible test for the fit of a model as we need to predict only one edge at a time. However, if one were to consider all edges in a cross-validation assessment, good link prediction performance indicates a good model fit for other structure in the data. Our higher-order link prediction task probes a larger set of features, in that it requires us to be able to predict more aspects of the data (any higher-order interaction, in principle).

For simplicity of presentation and scalability reasons, we predict simplicial closure events on triples of nodes. Thus, the higher-order link prediction problem examined here is predicting which triples of nodes that have not yet appeared in a simplex together will be a subset of some simplex in the future. Our above analysis suggests that open triangles or triples of nodes with strong ties are the most likely to close in the future. For our experiments, we predict which open triangles will go through a simplicial closure event in the future. Thus, this is a problem completely ignored by traditional link prediction, which would just view the triangle as already part of the graph. From a computational view, this restriction also makes it feasible to enumerate all open structures upon which the algorithms will make a prediction, using only modest computational resources. Thus, we avoid a common problem in link prediction of how to pare down an enormous candidate set of potential links, which itself is an active research topic (43, 44).

Simple local features predict well. We first split the data into training (first 80% of simplices in time) and test (final 20%) sets. Then, we evaluated the prediction performance of several new models (several inspired from classical link-prediction) on each dataset by the area under the precision-recall curve (AUC-PR) metric (Table 3). We use random scores as a baseline, which, with respect to AUC-PR, corresponds to the proportion of open triangles in the training set that go through a simplicial closure event in the test set.

We compare eight models here and provide additional comparisons in *SI Appendix*. Three are heuristics based on our finding that tie strength is indicative of closure; these are the harmonic, geometric, and arithmetic means of the three edge weights in the open triangle. Two more are based on the Adamic-Adar model (45) and the preferential attachment model. The latter has been suggested as a growth mechanism of coauthorship networks (20, 34). Two are based on longer path counts (Katz and personalized PageRank), which are models known for providing good prediction in dyadic link prediction (32). Lastly, we use a supervised logistic regression model based on features from the other models.

No single model performs the best over all datasets, but our proposed baseline algorithms can achieve much better performance than randomly guessing which open triangles go through a simplicial closure event. In the threads datasets, we achieve between one and two orders of magnitude performance improvements with the harmonic and geometric means, which indicates that local tie strength is relatively more important for these datasets than others. The absolute performance of the algorithms is far from perfect (see *SI Appendix*), as the higher-order link prediction is challenging. This finding is consistent with recent research on subgraph prediction in

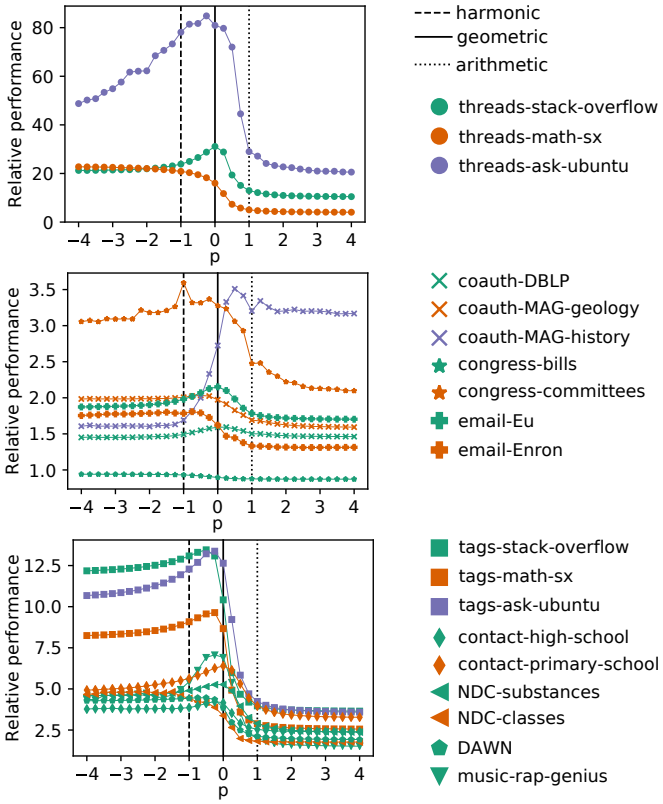

Fig. 7. AUC-PR relative to random predictions as a function of the parameter p in the generalized mean heuristic model for higher-order link prediction.

pairwise networks (46). However, our goal here is to identify some of the important structural features of the problem, rather than to predict with perfect accuracy.

The harmonic and geometric means of edge weights perform well across many datasets, which further highlights the importance of tie strength in predicting simplicial closure events. This finding is fundamentally different from traditional link prediction with pairwise interactions (i.e., for the edges in a graph). In traditional link prediction, a key principle is that it is valuable to use information contained in paths of non-trivial length between two nodes u and v for predicting a link between them—for example, PageRank and Katz measures are effective (32, 33). In this sense, higher-order link prediction is fundamentally more local in its overall structure. This arises from the ability of a k-tuple of nodes, for $k \geq 3$, to contain rich local information in its interactions among subsets of size $k-1$, a phenomenon that has no natural analogue when $k = 2$.

The arithmetic mean performs the worst of the three means in all but one dataset. We further analyze the performance of edge weight means using the generalized mean with parameter p as score functions: $s_p(u, v, w) = [(W_{uv}^p + W_{uw}^p + W_{vw}^p)/3]^{1/p}$, where W_{ab} is the weight between nodes a and b in the projected graph. The harmonic, arithmetic, and geometric means are the special cases where $p = -1$, $p = 1$, and the limit $p \to 0$. Generally, prediction performance is (i) unimodal in p, (ii) maximized for $p \in [-1, 0]$, and (iii) better for $p < -1$ than for $p > 1$ (Fig. 7). Two exceptions are NDC-classes and coauth-MAG-History. The former is the only dataset without an open triangle with exactly one strong tie to close. Thus, smaller p should perform better, as this accounts more for the minimum edge weight value. The latter is the dataset with the smallest average degree in the projected graph (Fig. 2C). Therefore, a single strong edge could provide the signal for closure, in which case a larger p is a better score function.

The supervised learning approach also performs well broadly, especially in the larger datasets such as the coauthorship datasets, which have sufficient training data to learn a good model. However, even when including the features of the other models, the method does not always perform the best. This is likely a case of overfitting (47). In the case of the congress bills data, the supervised method captures a unique feature of this dataset—nodes appearing in fewer simplices are *more* likely to go through a simplicial closure event. This is possibly due to the ambition of junior Congresspersons. The fact that combinations of features prove effective in many domains highlights the richness of the underlying problem, and the array of methods and findings presented here can guide progress on better models.

Discussion

The dyadic network modeling paradigm has been successful but fails to capture natural higher-order interactions. Here, we established the foundation for analyzing the basic structure of temporal networks with higher-order structure. We found rich structural variety in our datasets in terms of the fraction of triangles that are open, the average degree, and the edge density. Local statistics at the level of egonets can identify system domain, which suggests that these features are key to the organizing principles of the systems. Recent research shows the small fraction of triangles that are open in coauthorship networks (28); our results are consistent but reveal that open triangles are extremely common in other domains. Prior research has also identified the distinction between open and closed triangles when projecting bipartite networks but have not studied the idea of simplicial closure events (7, 48).

We found that common principles from dyadic network evolution also hold for higher-order structure, namely, tie strength and edge density are positive indicators of simplicial closure events amongst sets of three and four nodes. However, there is tension between these features—the more influential feature depends on the dataset, suggesting different mechanisms for simplicial closure events. For example, edge density matters more in human interaction, but tie strength matters more for tagging on online discussion platforms.

Higher-order link prediction provides a general methodology for evaluating models in any data where higher-order structure evolves over time, such as predicting which sets of authors will write a paper together or which sets of people will appear as joint recipients on an email. We anticipate that higher-order link prediction will validate emerging higher-order network modeling techniques, such as multipartite networks (49), meta paths (50), embeddings (51), and connect to ideas in computational topology, such as random walks on simplicial complexes (52, 53). Related higher-order models for different data (18, 19) can also use higher-order link prediction for model evaluation. For example, in the absence of temporal information, higher-order link prediction could be used to find missing data, similar to how dyadic link prediction can find missing data in static networks (35). Our higher-order link prediction framework also provides a way to study more sophisticated models where the underlying network is also dynamic, e.g., with arrival and departure of nodes. Specifically, such models should be able to predict higher-order links.

Our prediction problem examined a structure that is not even considered in traditional network analysis, where no distinction is made between open and closed triangles. From this setup, we found that simple local measures (generalized means of edge weights) are effective predictors. This finding differs from traditional link prediction, where long paths are important (32) and suggests that the temporal evolution of higher-order network data is fundamentally different than dyadic network evolution.

Materials and Methods

System domain prediction from egonet statistics. We computed (i) the fraction of open triangles, (ii) the log of the average degree in the projected graph, and (iii) the log of edge density in the projected graph of 100 egonets sampled uniformly at random (without replacement) from all egonets containing at least one open or closed triangle in each of 13 datasets categorized as coauthorship, stack exchange tags, stack exchange threads, email, or contact. Using 80 samples from each of the 13 datasets as training data, we trained an ℓ_2-regularized multinomial logistic regression classifier to predict the system domain given the three features above and an intercept term. The model was trained using the scikit-learn library (the regularization parameter was set to $C = 10$). Test accuracy was computed on the remaining 20 samples for each dataset. This entire process described was repeated 20 times, resulting in 20 different collections of egonet samples. Table 2 reports the mean and standard deviation of test accuracy over the 20 trials. The decision boundary in Fig. 3 comes from one of the 20 trials. Finally, let p_c be the fraction of egonets in a system domain within the training data and C the set of all classes. Then random guessing accuracy is $\sum_{c \in C} p_c^2$. The square appears because class c appears in a p_c fraction of the data and is guessed correctly with probability p_c.

Hypothesis testing for simplicial closure event probabilities. Let n_c and x_c denote the number of instances of an open configuration c in the training set (first 80% of data) and the number of those instances that close in the test set (final 20% of data). For a pair of configurations c and c', we use a one-sided hypothesis test for $x_c/n_c < x_{c'}/n_{c'}$. We use Fisher's exact test when $\max(x_c, x_{c'}) \leq 5$; otherwise, we use a one-sample z-test.

Data and software. Data collection details are in *SI Appendix*. Datasets are available at http://www.cs.cornell.edu/~arb/data/. Software is available at https://github.com/arbenson/ScHoLP-Tutorial.

ACKNOWLEDGMENTS. We thank Mason Porter and Peter Mucha for providing the Congress committees dataset. We thank Paul Horn, Gabor Lippner, and Jarosław Błasiok for helpful discussion. This research was supported in part by a Simons Investigator Award. RA was supported in part by a Google scholarship and a Facebook scholarship. AJ received funding from the Vannevar Bush Fellowship from the office of the Secretary of Defense. MTS received funding from the European Union's Horizon 2020 research and innovation programme under the Marie Sklodowska-Curie grant agreement No 702410.

1. Albert R, Barabási AL (2002) Statistical mechanics of complex networks. *Reviews of Modern Physics* 74(1).
2. Easley D, Kleinberg J (2010) *Networks, crowds, and markets: Reasoning about a highly connected world.* (Cambridge University Press).
3. Newman MEJ (2003) The structure and function of complex networks. *SIAM Rev* 45(2).
4. Granovetter MS (1973) The strength of weak ties. *Am. J. Sociol.* 78(6).
5. Deane CM, Salwiński Ł, Xenarios I, Eisenberg D (2002) Protein interactions: two methods for assessment of the reliability of high throughput observations. *Mol. & Cell. Proteomics* 1(5).
6. Bullmore E, Sporns O (2009) Complex brain networks: graph theoretical analysis of structural and functional systems. *Nature Reviews Neuroscience* 10(3).
7. Newman MEJ, Watts DJ, Strogatz SH (2002) Random graph models of social networks. *Proc. Natl. Acad. Sci.* 99(Suppl.1).
8. Milo R, et al. (2002) Network motifs: simple building blocks of complex networks. *Science* 298(5594).
9. Ugander J, Backstrom L, Marlow C, Kleinberg J (2012) Structural diversity in social contagion. *Proc. Natl. Acad. Sci.* 109(16).
10. Benson AR, Gleich DF, Leskovec J (2016) Higher-order organization of complex networks. *Science* 353(6295).
11. Grilli J, Barabás G, Michalska-Smith MJ, Allesina S (2017) Higher-order interactions stabilize dynamics in competitive network models. *Nature*.
12. Navlakha S, Kingsford C (2010) The power of protein interaction networks for associating genes with diseases. *Bioinformatics* 26(8).
13. Frankl P (1995) Extremal set systems in *Handbook of combinatorics*, eds. Graham R, Groetschel M, Lovasz L. (Elsevier) Vol. 1.
14. Berge C (1989) *Hypergraphs.* (Elsevier).
15. Hatcher A (2002) *Algebraic topology.* (Cambridge University Press).
16. Feld SL (1981) The focused organization of social ties. *Am. J. Sociol.* 86(5).
17. Kivelä M, et al. (2014) Multilayer networks. *Journal of complex networks* 2(3):203–271.
18. Xu J, Wickramarathne TL, Chawla NV (2016) Representing higher-order dependencies in networks. *Science Advances* 2(5).
19. Rosvall M, Esquivel AV, Lancichinetti A, West JD, Lambiotte R (2014) Memory in network flows and its effects on spreading dynamics and community detection. *Nature Comms.* 5(1).
20. Newman MEJ (2001) Clustering and preferential attachment in growing networks. *Physical Review E* 64(2).
21. Porter MA, Mucha PJ, Newman MEJ, Warmbrand CM (2005) A network analysis of committees in the U.S. House of Representatives. *Proc. Natl. Acad. Sci.* 102(20).
22. Fowler JH (2006) Legislative cosponsorship networks in the US house and senate. *Soc. Networks* 28(4).
23. Klimt B, Yang Y (2004) The Enron Corpus: A New Dataset for Email Classification Research in *Machine Learning: ECML 2004.* (Springer Berlin Heidelberg), pp. 217–226.
24. Paranjape A, Benson AR, Leskovec J (2017) Motifs in temporal networks in *Proceedings of WSDM.* pp. 601–610.
25. Mastrandrea R, Fournet J, Barrat A (2015) Contact patterns in a high school: A comparison between data collected using wearable sensors, contact diaries and friendship surveys. *PLOS ONE* 10(9):e0136497.
26. Stehlé J, et al. (2011) High-resolution measurements of face-to-face contact patterns in a primary school. *PLOS ONE* 6(8):e23176.
27. Kossinets G, Watts DJ (2006) Empirical analysis of an evolving social network. *Science* 311(5757).
28. Patania A, Petri G, Vaccarino F (2017) The shape of collaborations. *EPJ Data Science* 6(1).
29. Bertrand G (2011) Completions and simplicial complexes in *Discrete Geometry for Computer Imagery.* (Springer Berlin Heidelberg), pp. 129–140.
30. Leskovec J, Backstrom L, Kumar R, Tomkins A (2008) Microscopic evolution of social networks in *Proceeding of KDD.*
31. Backstrom L, Huttenlocher D, Kleinberg J, Lan X (2006) Group formation in large social networks: membership, growth, and evolution in *Proceedings of KDD.*
32. Liben-Nowell D, Kleinberg J (2007) The link-prediction problem for social networks. *Journal of the American Society for Information Science and Technology* 58(7):1019–1031.
33. Lü L, Zhou T (2011) Link prediction in complex networks: A survey. *Physica A: Statistical Mechanics and its Applications* 390(6).
34. Barabási A, et al. (2002) Evolution of the social network of scientific collaborations. *Physica A: Statistical Mechanics and its Applications* 311(3-4):590–614.
35. Clauset A, Moore C, Newman MEJ (2008) Hierarchical structure and the prediction of missing links in networks. *Nature* 453(7191).
36. Grover A, Leskovec J (2016) node2vec: Scalable feature learning for networks in *Proceedings of KDD.*
37. Santolini M, Barabási AL (2018) Predicting perturbation patterns from the topology of biological networks. *Proc. Natl. Acad. Sci.* 115(27).
38. Backstrom L, Leskovec J (2011) Supervised random walks: Predicting and recommending links in social networks in *Proceedings of WSDM.*
39. Wang X, Gulbahce N, Yu H (2011) Network-based methods for human disease gene prediction. *Briefings in Functional Genomics* 10(5).
40. Tang J, Wu S, Sun J, Su H (2012) Cross-domain collaboration recommendation in *Proceedings of KDD.*
41. Ghasemian A, Hosseinmardi H, Clauset A (2018) Evaluating overfit and underfit in models of network community structure. *arXiv:1802.10582.*
42. Kawamoto T, Kabashima Y (2017) Cross-validation estimate of the number of clusters in a network. *Scientific reports* 7(1):3327.
43. Ballard G, Kolda TG, Pinar A, Seshadhri C (2015) Diamond sampling for approximate maximum all-pairs dot-product (MAD) search in *Proceedings of ICDM.*
44. Sharma A, Seshadhri C, Goel A (2017) When hashes met wedges: A distributed algorithm for finding high similarity vectors in *Proceedings of WWW.*
45. Adamic LA, Adar E (2003) Friends and neighbors on the web. *Soc. Networks.*
46. Meng C, Mouli SC, Ribeiro B, Neville J (2018) Subgraph pattern neural networks for high-order graph evolution prediction. *AAAI Conference on Artificial Intelligence.*
47. Friedman J, Hastie T, Tibshirani R (2001) *The elements of statistical learning.* (Springer series in statistics New York, NY, USA:) Vol. 1.
48. Opsahl T (2013) Triadic closure in two-mode networks: Redefining the global and local clustering coefficients. *Soc. Networks* 35(2).
49. Lind PG, Herrmann HJ (2007) New approaches to model and study social networks. *New Journal of Physics* 9(7).
50. Sun Y, Han J, Aggarwal CC, Chawla NV (2012) When will it happen?: relationship prediction in heterogeneous information networks in *Proceedings of WSDM.*
51. Goyal P, Ferrara E (2017) Graph embedding techniques, applications, and performance: A survey. *arXiv preprint 1705.02801.*
52. Mukherjee S, Steenbergen J (2016) Random walks on simplicial complexes and harmonics. *Random Structures & Algorithms* 49(2).
53. Parzanchevski O, Rosenthal R (2016) Simplicial complexes: Spectrum, homology and random walks. *Random Structures & Algorithms* 50(2).